Synthesis, growth and characterization of nonlinear optical single crystal: glycine ammonium chloride

N. NITHYA[a], R. MAHALAKSHMI[b] , S. SAGADEVAN[c*]
[a]*Department of Physics, Sree Sastha College of Engineering, Chembarambakkam, Chennai, 600 123, India*
[b]*Department of Physics, GKM College of Engineering and Technology, Chennai-600 063, India*
[c*]*Department of Physics, AMET University, Kanathur, Chennai-603 112, India*

Nonlinear optical single crystals of Glycine Ammonium Chloride (GAC) have been grown by slow evaporation method. The lattice parameters and crystal system of the grown crystals were confirmed by single crystal X-ray diffraction analysis. Fourier transform infrared (FTIR) analysis confirms the various functional groups present in the grown crystal. The thermal behavior of the grown crystal was investigated by DTA and TGA analysis. The optical properties of the crystals were determined using UV-Visible spectrum. Optical constants such as band gap, refractive index, reflectance, extinction coefficient and electric susceptibility were determined from UV-Visible spectrum. The mechanical properties of the grown crystals were studied using Vickers microhardness tester. The second harmonic generation (SHG) test has been confirmed by the Kurtz powder test. The dielectric constant and dielectric loss of the crystal are studied as a function of frequency for different temperatures. The photoconductivity studies confirm that the grown crystal has negative photoconductivity nature. In order to investigate the growth mechanism and surface features, etching studies are carried out for the crystal.

(Received March 15, 2015; accepted February 10, 2016)

Keywords: Single X-ray diffraction, UV-Vis-NIR spectrophotometer, NLO, SHG, Dielectric constant and Dielectric loss

1. Introduction

Nonlinear optical applications require good quality single crystals which succeed to large NLO coefficient coupled with enhanced physical parameters. One potentially attractive system, where there is a potential for realizing enormous second order nonlinear coefficient is based on organic crystals. Organic materials have been of particular attention because the nonlinear optical responses in this wide class of materials is microscopic in origin, offering an opportunity to use theoretical modeling coupled with synthetic flexibility to design and produce novel materials. Further investigations on organic NLO materials have subsequently created great materials with extremely attractive characteristics. Nonlinear optical process gives the key function of frequency conversion and optical switching [1-3]. The different properties of the materials, such as transparency, birefringence, refractive index and chemical stability depends on these characteristics. Organic nonlinear materials are attracting a big deal of attention, as they have huge optical susceptibilities, inherent ultra fast response time and high optical threshold laser power as compared with inorganic materials [4]. Moreover, amino acids are dipolar in nature and the molecules have an electron donor group and an electron acceptor group. This leads to large second order optical nonlinearity arising out of intramolecular charge transfer between the donor and acceptor. Due to dipolar nature, amino acids are measured to be high potential for NLO applications. Materials with large second-order optical nonlinearities, short transparency cut off wavelengths and stable physicochemical performances are required to realize the applications on the basis of optical storage devices [5]. Among organic NLO materials, amino acids display specific features such as molecular chirality, absence of strongly conjugated bonds and zwitter ionic nature of the molecule. Further, amino acids contain a proton-donor carboxyl (-COO) group and the proton-acceptor amino ($-NH_2$) group in them and thereby creating "push – pull" type motif to enhance the NLO response. Glycine is the simplest amino acid. Glycine remains as one of the most extensively studied amino acids as it is known to form innumerable complexes with metals, inorganic salts and inorganic acids. Many researchers have investigated the properties of pure glycine and its derivatives. The present investigation deals with the growth of glycine ammonium chloride (GAC) single crystal that was grown by slow evaporation technique. The grown crystals were characterized by single crystal X-ray analysis, FTIR, thermal analysis UV spectral analysis, microhardness, dielectric, SHG, photoconductivity measurements and etching studies.

2. Experimental procedure

Glycine ammonium chloride was grown from glycine and ammonium chloride in equimolar ratio in aqueous solution by slow evaporation method. The solution was stirred continuously using a magnetic stirrer. The prepared solution was filtered and kept undisturbed at room temperature. Tiny seed crystals with good transparency were obtained due to spontaneous nucleation. Among them, defect free seed crystal was selected and suspended

in the mother solution, which was allowed to evaporate at room temperature. Large size single crystals were obtained due to the collection of monomers at the seed crystal sites from the mother solution, after the nucleation and growth processes were completed. GAC crystal of dimension about 11 x 7 x 8 mm^3 was harvested in a growth period of twenty four days by slow evaporation of the solvent. The photograph of the grown GAC crystal is shown in Fig. 1.

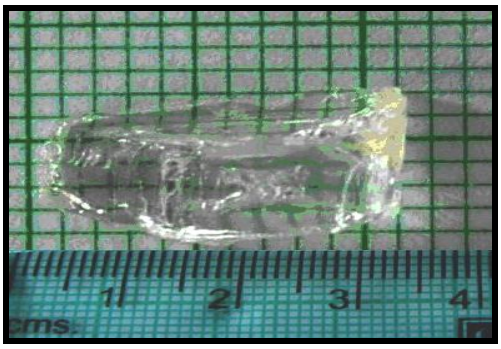

Fig.1. Photograph of grown GAC single crystal.

3. Results and discussion

3.1. Single-crystal X-Ray diffraction

The single-crystal X-ray diffraction analysis of the grown crystals was carried out to identify the cell parameters using an ENRAF NONIUS CAD4 automatic X-ray diffractometer. From the single crystal X-ray diffraction analysis, it is observed that the GAC crystal is hexagonal in structure. The lattice parameters were calculated to be a = 6.532 Å, b = 6.583 Å, c = 5.325 Å, which agrees well with the available reported values [6].

3.2 FTIR spectrum analysis

FTIR spectrum is significant evidence that gives more information about the structure of a compound. In this technique, almost all functional groups in a molecule absorb characteristically within a definite range of frequency. The absorption of IR radiation causes the various bonds in the molecule to stretch and bend with respect to one another. The most important range (4000 - 400 cm^{-1}) is of prime importance for the study of an organic compound by spectral analysis. In the present study FTIR spectrum was recorded using BRUKER IFS 66V spectrometer with KBr pellet technique. The spectrum of GAC is shown in Fig.2. The frequencies observed at 3092 and 2727cm^{-1} are attributed to NH_3^+ stretching and C-H stretching respectively. The absorption peaks observed at 1013 cm^{-1} respond to C-C-N group. The peaks observed at 1325 cm^{-1} is attributed to CH_2 group while the peak observed at 1585 cm^{-1} is attributed to COO^- group. The analysis of the spectrum shows amino acid characteristics and the results agree very well with the already reported prediction [6].

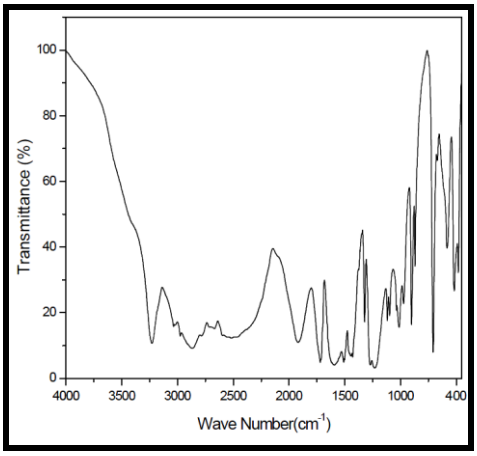

Fig.2. FTIR spectrum of the grown crystal GAC.

3.3 Thermal studies

DTA and TGA analysis were carried out with the help of instrument TG/DTA 6200 simultaneous thermal analyzer. Thermal analyzer and the resulting thermogram and its differential thermogravimetric curves are shown in Fig.3. The weight loss of about 35% between 104°C and 148°C is attributed to the loss of lattice water. There is a small weight loss at 195˚ C to 255˚ C. There is a sharp weight loss at 255˚ C without any intermediate stages and this is assigned as the melting point of the crystal. This study indicates that the compound could be used for device fabrication below its melting point of the crystal. The resulting residue gives a weight loss for a wider range of temperature between 50°C and 300°C. The DTA thermogram also reveals that the sharp exothermic peak coincides with that of TG confirms the thermal stability of the crystal. The endothermic peaks of the DTA trace are observed to coincide with the decomposition in the TGA trace. From this study, it can be concluded that the crystal can retain texture upto 195ºC. The obtained results are in good agreement with the earlier reports [6].

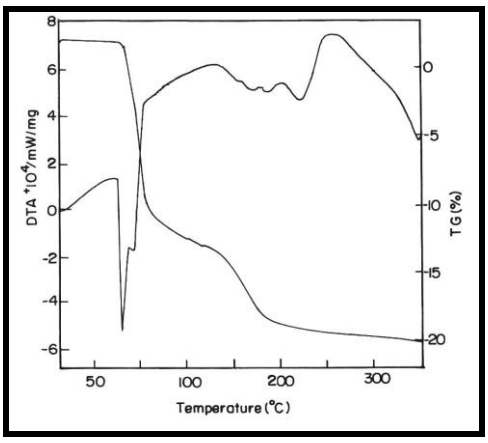

Fig.3. TGA and DTA thermograms of GAC crystal.

3.4 UV-Vis-NIR spectral analysis

The optical transmission spectrum of GAC single crystal was recorded in the wavelength region 200 – 1000 nm using PERKIN ELMER LAMDA Instrument and it is shown in Fig.4. For optical fabrications, the crystal should be highly transparent in the considered region of wavelength [7, 8]. The favorable transmittance of the crystal in the entire visible region suggests its suitability for second harmonic generation [9]. The UV absorption edge for the grown crystal was observed to be around 245 nm. The dependence of optical absorption coefficient on photon energy helps to study the band structure and type of transition of electrons [10].

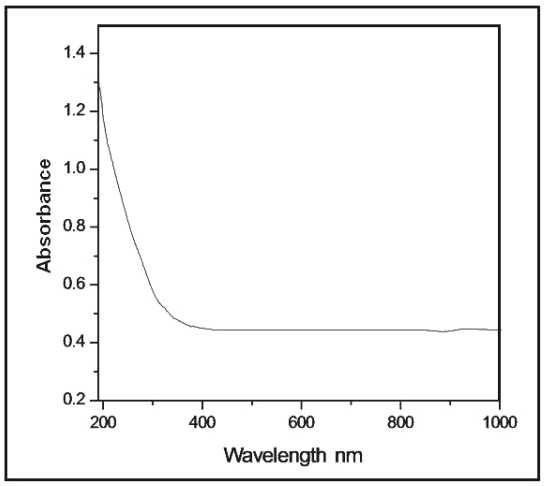

Fig.4 UV-Visible absorbance spectrum of GAC crystal.

The optical absorption coefficient (α) was calculated from transmittance using the following relation

$$\alpha = \frac{1}{d} Ln\left(\frac{1}{T}\right) \tag{1}$$

where T is the transmittance and d is the thickness of the crystal. As a direct band gap material, the crystal under study has an absorption coefficient (α) obeying the following relation for high photon energies (hν)

$$\alpha = \frac{A(h\nu - E_g)^{1/2}}{h\nu} \tag{2}$$

where E_g is the optical band gap of the crystal and A is a constant. A plot of variation of $(\alpha h\nu)^2$ versus hν is shown in Fig.5. E_g is evaluated using the extrapolation of the linear part [11]. Using Tauc's plot, the energy gap (E_g) was calculated as 5.07 eV. This high band gap value indicates that the grown crystal possesses dielectric behaviour to induce polarization when powerful radiation is incident on the material.

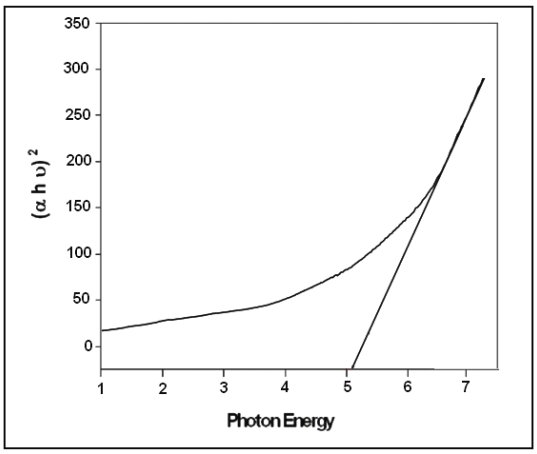

Fig.5. Plot of $(\alpha h\nu)^2$ Vs photon energy .

3.4.1 Determination of optical constants

Two of the most important optical properties; refractive index and the extinction coefficient are generally called optical constants. The amount of light that transmitted through crystal depends on the amount of the reflection and absorption that takes place along the light path. The optical constants such as the refractive index (n), the real dielectric constant (ε_r) and the imaginary part of dielectric constant (ε_i) were determined using UV-Visible spectrum. The extinction coefficient (K) can be obtained from the following equation,

$$K = \frac{\lambda\alpha}{4\pi} \tag{3}$$

The extinction coefficient (K) was found to be 3.12 x 10^{-6} at λ =1000 nm. The transmittance (T) is given by

$$T = \frac{(1-R)^2 \exp(-\alpha t)}{1-R^2 \exp(-2\alpha t)} \tag{4}$$

Reflectance (R) in terms of absorption coefficient can be obtained from the above equation. Hence,

$$R = \frac{1 \pm \sqrt{1-\exp(-\alpha t + \exp(\alpha t)}}{1+\exp(-\alpha t)} \tag{5}$$

Refractive index (n) can be determined from reflectance data using the following equation,

$$n = -\frac{(R+1) \pm \sqrt{3R^2+10R-3}}{2(R-1)} \tag{6}$$

The refractive index (n) was found to be 1.62 at λ=1000 nm. From the optical constants, electric susceptibility (χ_c) can be calculated according to the following relation

$$\varepsilon_r = \varepsilon_0 + 4\pi\chi_C = n^2 - k^2 \tag{7}$$

Hence,

$$\chi_C = \frac{n^2 - k^2 - \varepsilon_0}{4\pi} \quad (8)$$

where ε_0 is the permittivity of free space. The value of electric susceptibility (χ_c) is 1.54 at λ=1000 nm. The real part dielectric constant (ε_r) and imaginary part dielectric constant (ε_i) can be calculated from the following relations [12]

$$\varepsilon_r = n^2 - k^2 \quad (9)$$

$$\varepsilon_i = 2nk \quad (10)$$

The value of real dielectric (ε_r) and imaginary constant (ε_i) at λ =1000 nm were estimated at 3.523 and 6.802 x 10^{-5}, respectively. The moderate values of refractive index and optical band gap suggest that the material has the required transmission range for NLO application. The lower value of dielectric constant and the positive value of the material are capable of producing induced polarization due to intense incident light radiation.

3.5 NLO test – Kurtz powder SHG method

The most widely used technique for confirming the SHG efficiency of NLO materials to identify the materials with non-centrosymmetric crystal structures is the Kurtz Powder technique [13]. In this technique the powdered sample with an average particle sizes range 125-150 μm is filled in a microcapillary tube about 1.5 mm diameter. Q-switched Nd:YAG laser emitting a fundamental wavelength of 1064 nm with an input power of 6.2 mJ/pulse and a pulse width of 8 ns with a repetition rate of 10 Hz was made to fall normally on the crystal. The output from the crystal was monochromated to collect the intensity of 532 nm component and to eliminate the fundamental wavelength. The second harmonic radiation generated by the randomly oriented micro crystals was focused by a lens and detected and a photo multiplier tube. The generation of the second harmonic was confirmed by a strong bright green emission emerging from the powdered crystal. A potassium dihydrogen phosphate (KDP) crystal was used as a reference material in the SHG measurement. The relative conversion efficiency was calculated from the output power of GAC crystals with reference to KDP crystals. It is observed that the conversion efficiency of GAC is 0.9 times that of KDP crystal.

3.6 Microhardness studies

Hardness of a material is the measure of resistance when it offers to local deformation. Indentations were made on (1 0 1) plane of GAC crystal using Shimadzu HMV-2000 fitted with Vickers pyramidal indenter. The microhardness measurements were carried out with a load range from 10 to 50 g. The Vickers microhardness number was calculated using the relation,

$$H_v = 1.8544\left(\frac{P}{d^2}\right) kg/mm^2 \quad (11)$$

where P is the indenter load and d is the diagonal length of the impression. The Fig.6 shows the variation of P with Vickers hardness number (H_v) for grown single crystal. It is evident from the plot that Vickers microhardness number increases with increasing applied load. According to Meyer's law, the relation connecting the applied load is given by

$$P = k_1 d^n \quad (12)$$

$$\log P = \log k + n \log d \quad (13)$$

where n is the Meyer index or work hardening exponent and k_1, is the constant for a given material. The above relation indicates that 'Hv' should increase with load P if n>2 and decrease with load P when n<2. We have determined 'n' from slope of the plot that is shown in Fig 7. The value of 'n' for GAC was found to be 3.2. According to Onitsch [14], 'n' should lie between 1 and 1.6 for harder materials and above 1.6 for softer materials. From the hardness study, the grown GAC crystal is found to be relatively soft material [15].

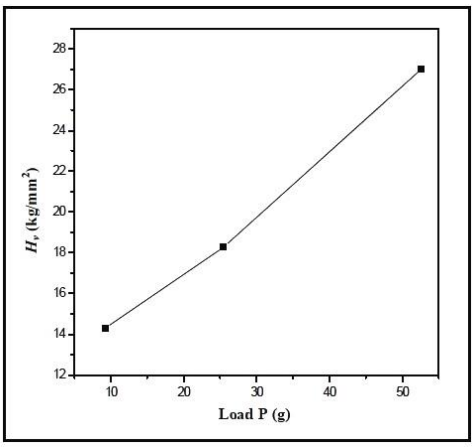

Fig.6 Variation of H_v with load P

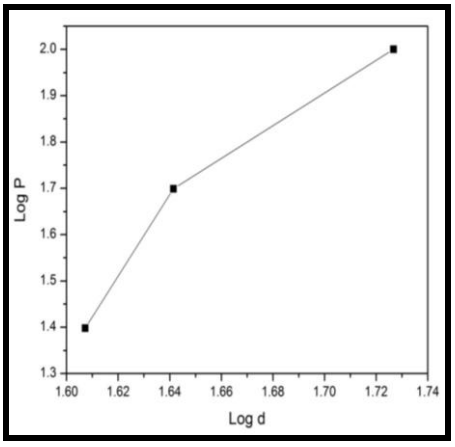

Fig.7. Plot of log d Vs log p.

3.7 Dielectric studies

Dielectric properties are related with the electric field distribution within solid materials. The dielectric study of GAC was carried out using the instrument, HIOKI 3532-50 LCR HITESTER. Good- quality crystals were selected

and polished by soft polishing pad with fine grade alumina powder. The face of single crystal was cut in to rectangular shape and well-polished, so that it behaves as a parallel plate capacitor. Silver paste was used for making the electrode plates on these surfaces of the crystal. The plots of dielectric constant and dielectric loss with frequency for various temperatures are shown in Figs 8 and 9. The dielectric constant is high in the lower frequency region and variation of dielectric constant with log f decreases with an increase in frequency. From the plot, it is also observed that dielectric constant increases with an increase in temperature. The high value of dielectric constant at low frequency may be due to presence of all polarizations and its low value at higher frequencies may be due to the significant loss of all polarizations gradually [16]. The variation of dielectric constant with temperature is generally attributed to the crystal expansion, the electronic and ionic polarizations and the presence of impurities and crystal defects. The dielectric loss was also studied as a function of frequency for different temperatures and is shown in Fig. 9. These curves suggest that the dielectric loss is strongly dependent on the frequency of the applied field. From the plot, it is also observed that dielectric loss increases with an increase in temperature. The behaviour of low dielectric loss with high frequency for the crystal suggests that the crystal possess enhanced optical quality with lesser defects and this parameter plays a vital role for the fabrication of nonlinear optical devices [17, 18].

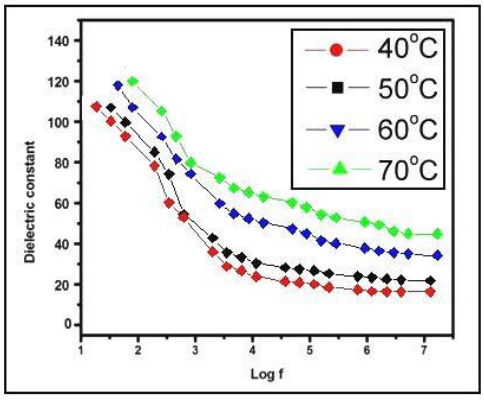

Fig.8. Variation of dielectric constant with log frequency.

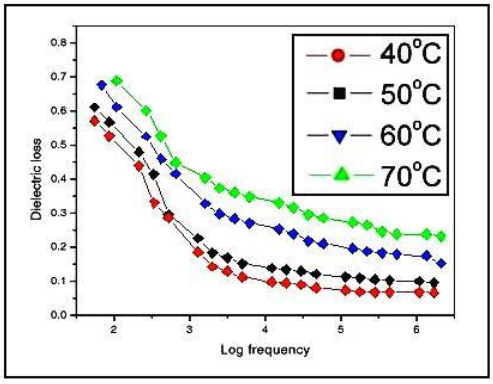

Fig. 9 Variation of dielectric loss with log frequency.

3.8 Photoconductivity studies

The GAC crystal is well-polished and surfaces are cleaned with acetone. This is attached to a microscope slide and two electrodes of thin copper wire (0.14 cm diameter) are fixed onto the specimen at some distance apart using silver paint. A DC power supply, a Keithley 485 picoammeter and the prepared crystal are connected in series. The crystal was covered with a black cloth and the dark current (I_d) of the crystal was recorded with respect to the different applied voltage. Then crystal was illuminated by the radiation from 100 W halogen lamp containing iodine vapour and tungsten filament and the corresponding photocurrent (Ip) is recorded for the same values of the applied voltage. The Fig.10 shows the variation of both dark current (I_d) and photocurrent (I_p) with the applied electrical field. In Stockmann's model, a two level scheme is proposed to explain negative photoconductivity [19]. The upper energy level is situated between the Fermi level and the conduction band, whereas the other one is located in the neighborhood of the valence band. The lower level has high capture cross-section for electrons from the conduction band and holes from the valence band. As a result, sooner the crystal is kept under exposed light, the recombination of electrons and holes take place, resulting in decrease in the number of mobile charge carriers, giving rise to negative photoconductivity. It is seen from the plots that both I_d and I_p of the crystal increase linearly with applied field. It is observed from the plot that the dark current is always higher than the photocurrent, thus confirming the negative photoconductivity nature of the GAC single crystal [20].

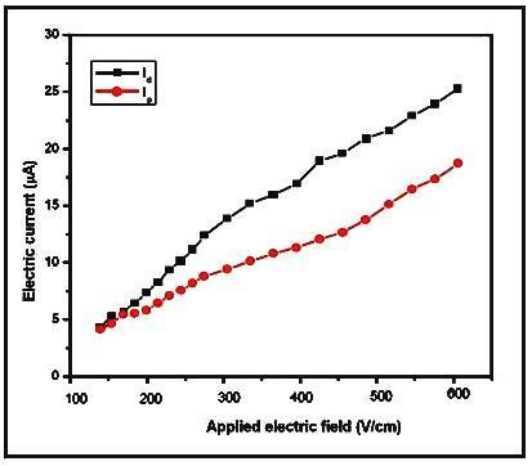

Fig.10. Field dependent photoconductivity of GAC crystal.

3.9 Etching studies

Etching is a technique which is used to reveal the defects in crystals like dislocations, growth bands, twin boundaries, point defects etc. Normally when the crystal is dissolved in the solvent, well defined etch pits are formed. Etching is one of the selective tools to identify the defects

in the as grown crystals [21]. Etching was carried out on the grown crystal of GAC. The shape of the etch pits depends on the lattice structure and symmetry of the crystal. Then the crystal was immersed in double distilled water for 10s.The crystal was clean and dried with immerse paper and once more observed under the optical microscope as shown in Fig. 11. From the fig, the rectangular ended elongated etch pits and striation was observed. The rectangular etch pit verify the growth of the crystal from 2D nucleation mechanism. The etch pits does not vanish upon etching show the presence of dislocations.

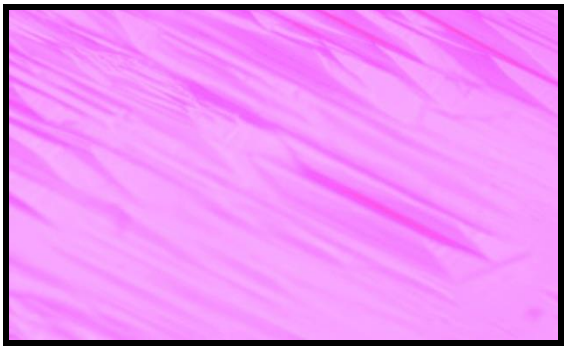

Fig. 11. Etch patterns observed of GAC.

4. Conclusion

A single crystal of GAC was grown by slow evaporation method. The cell parameters of the crystal were determined using single crystal X-ray diffraction analysis. The functional groups were confirmed from FTIR analysis. The thermal stability of the materials was established by TG/DTA and it is observed that the material is stable up to 195º C. The optical property of the grown material is studied by UV-Visible spectrum which shows the UV cut off wavelength to be 245 nm. The optical constant such as band gap, refractive index, reflectance, extinction coefficient and electrical susceptibility were calculated to analyze the optical property. Vickers microhardness was calculated in order to understand the mechanical stability of the grown crystals. The NLO property of the crystal was examined by performing Kurtz powder test using Nd: YAG laser. The variation of dielectric constant and dielectric loss was studied with varying frequency at different temperatures. The photoconductivity studies confirm that this material has negative photoconductivity nature. The etching studies were carried to study the formation of etch pits in water solvent.

References

[1] P.N. Prasad, D.J. Williams, Introduction to Non Linear Optical Effect in Molecules and Polymers, John Wiley & Sons, New York, (1991).
[2] D.S. Chemla, J. Zyss, (Eds). Non linear Optical Properties of Organic Molecules and Crystals, Academic press, New York, (1987).
[3] A. Datta, S.K. Pati, J. Chem. Phys.**118**, 8420-7 (2003).
[4] T. Pal, T. Kar, G. Bocelli, L. Rigi, Cryst. Growth. Des. **3,** 13 (2003).
[5] X.Q. Wang, D. Xu, M.K. Lu, D.T. Yuan, J. Huang, S.G. Li, G.W. Lu, H.Q. Sun, S.Y. Guo, G.H. Zhang, X.L. Duan, H.Y. Liu, W.L. Liu, J. Cryst. Growth. **247,** 432 (2003).
[6] M. Radha Ramanan , R. Radhakrishnan , S. Krishnan, V. Chithambaram, International Journal of Engineering Research & Technology (IJERT), **2,** 1 (2013).
[7] S. Suresh, D. Arivuoli, Journal of Minerals & Materials Characterization & Engineering, **10,** 517 (2011).
[8] S. Suresh, D. Arivuoli, Growth, Journal of Minerals & Materials Characterization & Engineering, **10,** 1131 (2011).
[9] S. Suresh, D. Arivuoli, Growth, Journal of Optoelectronics and Biomedical Materials. **3**, 63(2011).
[10] K. Pandurangan, S. Suresh, Journal of Materials, Art. ID 362678 (2014)
[11] S. Suresh, K. Anand, Advances in Applied Science Research **3,** 815 (2012).
[12] S. Sagadevan, P. Murugasen, Journal of Crystallization Process and Technology, **4,** 99 (2014).
[13] S.K. Kurtz, T.T. Perry, J.Appl.Phys. **39**, 3798 (1968).
[14] E.M. Onitsch, Microscope, **95**, 12(1950).
[15] S. Suresh, A. Ramanand, P. Mani, K. Anand, Journal of optoelectronics and biomedical materials **1,** 129 (2010).
[16] C.P. Smyth, Dielectric behaviour and structure, McGraw-Hill, New York, (1965).
[17] C.Balarew, R.Duhlev, J. Solid State Chem., **55,** 1(1984).
[18] S. Sagadevan, Optik - Int. J. Light Electron Opt. **125,** 6746 (2014).
[19] V.N. Joshi, Photoconductivity, Marcel Dekker, New York, (1990).
[20] S. Sagadevan, International Journal of ChemTech Research, **6,** 2645 (2014).
[21] Natarajan Nithya, Raman Mahalakshmi, Suresh Sagadevan, Materials Research. **18**(3), 581(2015).

*Corresponding author: sureshsagadevan@gmail.com